

Reperfusion Hemorrhage Following Acute Myocardial Infarction: Assessment with T2* Mapping and Effect on Measuring the Area at Risk¹

Declan P. O'Regan, FRCR, PhD
Rizwan Ahmed, MRCP
Narayan Karunanithy, FRCR
Clare Neuwirth, RN
Yvonne Tan, RN, BA
Giuliana Durighel, BSc
Joseph V. Hajnal, PhD
Imad Nadra, MRCP
Simon J. Corbett, PhD, MRCP
Stuart A. Cook, PhD, MRCP

Research ethics committee approval and informed consent were obtained. The purpose of this study was to assess the feasibility of multiecho T2* mapping of the heart for detecting reperfusion hemorrhage following percutaneous primary coronary intervention (PPCI) for acute myocardial infarction, and to measure the effect of hemorrhage on quantifying the ischemic area at risk (IAR) on T2-weighted magnetic resonance images. Fifteen patients (mean age, 59 years; 13 men, two women) were imaged a mean of 3.2 days following PPCI. The mean area of hemorrhage, indicated by a T2* decay constant of less than 20 msec, was $5.0\% \pm 4.9$ (standard deviation) at the level of the infarct and this correlated with the infarct ($r^2 = 0.76$, $P < .01$) and microvascular obstruction ($r^2 = 0.75$, $P < .01$) volumes. When 5% or less hemorrhage was present, the IAR was underestimated by 50% at a standard deviation threshold level of five, compared with a boundary detection tool (21.8% vs 44.0%, $P < .05$). T2* mapping is feasible for quantifying post-reperfusion hemorrhage and boundary detection is required to accurately assess the IAR when hemorrhage is present.

© RSNA, 2009

¹ From the Medical Research Council Clinical Sciences Centre, Faculty of Medicine, Imperial College, Hammer-smith Hospital Campus, Du Cane Road, London W12 0NN, England (D.P.O., R.A., C.N., Y.T., G.D., J.V.H., S.A.C.); National Heart and Lung Institute, Imperial College, London, England (S.A.C.); Department of Imaging, Imperial College Healthcare National Health Service (NHS) Trust, London, England (D.P.O., N.K.); and Department of Cardiology, Imperial College Healthcare NHS Trust, London, England (I.N., S.A.C., S.J.C). Received July 10, 2008; revision requested August 18; revision received August 29; accepted September 17; final version accepted September 18. Supported in part by the Medical Research Council, London, England; the British Heart Foundation, London, England; the Department of Health, London, England; the National Institute for Health Research Biomedical Research Centre, London, England; and the Fondation Leducq, Paris, France. Address correspondence to D.P.O. (e-mail: declan.oregan@csc.mrc.ac.uk).

© RSNA, 2009

Occlusion of a coronary artery leads to myocardial tissue edema in the vascular bed downstream of the vessel (1–3). This develops after an hour of occlusion or more (4) and may persist for several months (5). The increase in mobile water content within ischemic myocardium causes a prolongation of T2 magnetic resonance (MR) relaxation (6,7). Therefore, the extent of hyperintense edema on T2-weighted MR images allows the ischemic area at risk (IAR) of injury to be retrospectively determined (6,8–11). This zone includes myocardium that is potentially salvageable following reperfusion, as well as irreversibly injured tissue (8). However, reperfusion of severely ischemic myocardium also leads to interstitial hemorrhage, which may be an important marker for irreversible microvascular damage (12,13). The effects of hemorrhage on T2 signal are complex, but between 1 and 7 days after reperfusion, paramagnetic effects appear to predominate (14). Signal voids have been observed within infarctions on gradient-echo MR images, which correspond to histologic evidence of hemorrhage (11,15). Therefore, cardiac T2*-weighted mapping has the potential to quantify the extent of myocardial hemorrhage and compare it with other indexes of ischemic injury. Furthermore, the paramagnetic effects of hemorrhage would also be expected to cause signal loss on T2-weighted spin-echo MR images, which may lead to a clinically important underestimation of the IAR by using signal intensity threshold level criteria.

In this study, we assessed the feasibility of using T2*-weighted mapping to quantify regions of myocardial hemorrhage following percutaneous primary

coronary intervention (PPCI) for acute myocardial infarction. We also hypothesized that myocardial hemorrhage would lead to an underestimation of the IAR on T2-weighted MR images by using conventional signal intensity threshold intensity level criteria.

Materials and Methods

Participants

This study was approved by the research ethics committee (Hammer-smith Hospital, Hampshire, England) and all patients gave written informed consent. We prospectively investigated 15 consecutive patients (13 men, two women; mean age, 59 years; range, 41–74 years) who had undergone PPCI within the previous 7 days. The inclusion criteria were men and women aged 18–85 years, who had an electrocardiographic diagnosis of acute ST-elevation myocardial infarction and coronary intervention within 10 hours of symptom onset. Exclusion criteria were contraindications to cardiac MR imaging ($n = 3$), previous myocardial infarction (MI) or heart failure ($n = 0$), clinical instability ($n = 2$), significant arrhythmias ($n = 0$), and pregnancy or lactation ($n = 0$). All patients presented within 24 hours of the onset of chest pain for treatment of a first myocardial infarction. The diagnosis of MI required ST-elevation of 1 mm or more in two contiguous electrocardiographic leads and chest pain onset within 12 hours of presentation (≤ 24 hours in the case of ongoing symptoms). Coronary angiography and PPCI were performed by means of a transfemoral or transradial approach to identify and perform angioplasty on the infarct-related artery. The

use of bare-metal or drug-eluting stents and abciximab (ReoPro; Eli Lilly, Indianapolis, Ind) was at the operator's discretion. All patients received antiplatelet therapy with aspirin, clopidogrel (Plavix; Bristol-Myers Squibb, New York, NY), and intravenous heparin before PPCI.

Cardiac MR Protocol

The cardiac MR examinations were performed with a 1.5-T imager (Achieva, Philips; Best, the Netherlands) by an MR technologist (G.D., with 5 years experience). The maximum gradient strength was 31 mT/m and the maximum slew rate was 200 mT/m/msec. A five-element cardiac phased-array coil was used for signal reception. Coil sensitivity-based uniformity correction was performed by using the constant-level-appearance algorithm by using a breath-hold reference image of the thorax (16).

Scout images were obtained and used to plan an axial stack of balanced steady-state free precession cine MR images in the left ventricular (LV) short-axis plane from base to apex by using the following parameters: repetition time msec/echo time msec, 3.0/1.5; voxel size, $2.0 \times 2.2 \times 8$ mm; flip angle, 60°; section thickness, 8 mm; intersection gap, 2 mm; bandwidth, 1250 Hz/pixel; and 20 cardiac phases. Myocardial edema was imaged by using a breath-hold black-blood T2-weighted turbo

Advances in Knowledge

- Navigator-gated T2*-weighted MR mapping can be used to image myocardial hemorrhage following infarct reperfusion.
- Myocardial hemorrhage leads to an underestimation of the ischemic area at risk (IAR) seen on T2-weighted MR images by using signal intensity threshold level criteria.

Implications for Patient Care

- Hemorrhage after reperfusion may be quantified and compared with other measures of ischemic injury.
- Boundary detection avoids underestimating the IAR seen at T2-weighted imaging in the presence of reperfusion hemorrhage.

Published online before print

10.1148/radiol.2503081154

Radiology 2009; 250:916–922

Abbreviations:

IAR = ischemic area at risk
 LV = left ventricle
 MVO = microvascular obstruction
 PPCI = percutaneous primary coronary intervention
 SD = standard deviation

Author contributions:

Guarantors of integrity of entire study, D.P.O., S.A.C.; study concepts/study design or data acquisition or data analysis/interpretation, all authors; manuscript drafting or manuscript revision for important intellectual content, all authors; approval of final version of submitted manuscript, all authors; literature research, D.P.O.; clinical studies, D.P.O., R.A., N.K., C.N., G.D., I.N., S.J.C.; experimental studies, N.K., G.D., I.N., S.A.C.; statistical analysis, D.P.O., N.K., S.A.C.; and manuscript editing, D.P.O., R.A., C.N., J.V.H., I.N., S.J.C., S.A.C.

Authors stated no financial relationship to disclose.

spin-echo sequence with short inversion time inversion recovery fat suppression with the following parameters: repetition time, two R-R intervals; echo time, 100 msec; voxel size, $1.9 \times 2.6 \times 10$ mm; flip angle, 90° ; section thickness, 10 mm; and bandwidth, 467 Hz/pixel.

Myocardial hemorrhage was imaged with a dual-inversion black-blood gradient multiecho T2* MR sequence by using the following parameters: 17/2.3–16.1; seven echoes obtained; change in echo time, 2.3 msec; voxel size, $1.7 \times 2.8 \times 10$ mm; flip angle, 20° ; section thickness, 10 mm; and bandwidth, 1387 Hz/pixel. A single short-axis image plane was chosen at the level of maximal edema. Cardiac triggering was set for mid diastole to reduce motion artifact. Localized volume shimming was used with a volume placed over the whole heart. Navigator echo respiratory gating was used to acquire images during free breathing with the pencil-beam excitation localized to the right hemidiaphragm.

An intravenous bolus of gadopentetate dimeglumine (Magnevist; Bayer Schering Pharma, Berlin, Germany) was administered at a dose of 0.2 mmol per kilogram of body weight by using a power injector (Spectris Solaris; Medrad, Indianola, Pa). Microvascular

obstruction (MVO) was imaged within 1 minute of contrast material injection by using a three-dimensional inversion-recovery breath-hold sequence with the following parameters: 4.3/1.4; inversion time, 180 msec; voxel, $1.4 \times 1.4 \times 8$ mm; flip angle, 15° ; section thickness, 8 mm; and bandwidth, 266 Hz/pixel. Infarct size was subsequently imaged in the same manner at 15 minutes following injection of contrast material, with the inversion time adjusted to null the signal from normal myocardium by using the Look-Locker method (17).

Cardiac MR Image Analysis

All cardiac MR measurements were performed independently by two observers (D.P.O. and S.A.C., each with 5 years experience in cardiac MR) and the mean value was used for analysis. Segmentation of the LV cavity and wall from the short-axis balanced steady-state free precession cine MR images was performed by using software (CMRtools; Cardiovascular Imaging Solutions, London, England). LV mass, end-diastolic volume, and end-systolic volume were calculated and indexed to body surface area. The T2-weighted short inversion time inversion recovery images were analyzed by

using software (Medical Image Processing, Analysis, and Visualization; National Institutes of Health, Bethesda, Md) (18). The images were first manually masked to include only the myocardium for subsequent analysis. This excluded any unsuppressed slow-flowing blood adjacent to the LV wall. The area of hyperintense myocardial edema, indicative of the IAR, was measured with semiautomated boundary segmentation by using the level-set method (19). Each observer defined a point at the edge of the hyperintense zone and a boundary was then automatically generated around the IAR. This method was compared with a conventional signal intensity threshold level method by using two, three, and five standard deviations (SDs) above the mean of remote normal myocardium (9). A pixel-by-pixel analysis was performed of the multiecho T2*-weighted images by using software (Matlab, version 2007a; Mathworks, Natick, Mass) with fitting to a simple monoexponential decay by using the following equation:

$$S(t) = S_0 e^{-TE/T2^*},$$

where S_0 is the initial magnitude signal

Figure 1



Figure 1: LV short-axis images acquired 2 days after PPCI of left anterior descending artery occlusion. **(a)** T2*-weighted MR imaging map (17/2.3–16.1; flip angle, 20° ; black-blood prepulse) acquired before contrast material administration. Pixels with T2* decay constant of less than 20 msec (red) show region of postreperfusion hemorrhage (arrow). Susceptibility artifact adjacent to inferolateral epicardium was manually excluded, if present (arrowhead). **(b)** Hemorrhage closely corresponds to area of MVO (red) shown on early enhancement image (4.3/1.4/180 and flip angle, 15°). **(c)** Extent of enhancing myocardial necrosis (red) and residual MVO (black core) is shown on late enhancement image (4.3/1.4/250 and flip angle, 15°).

intensity, $S(t)$ is the magnitude of signal intensity at TE, echo time, and $T2^*$ is the decay constant. Hemorrhage was considered to be present if the $T2^*$ value was below the normal myocardial value of 20 msec reported in healthy subjects (20) and was expressed as a percentage of LV area of that section. Susceptibility artifact adjacent to the inferolateral LV epicardium was excluded, if present (21,22). The volume of myocardial hypointensity on the early enhancement images was

used to define percentage of MVO, and the volume of hyperintensity, including residual MVO, on the late enhancement images was used to define infarct percentage. A salvage index was calculated as the proportion of the IAR that did not show late enhancement.

Statistical Analysis

All continuous data are reported as the mean \pm SD. The Mann-Whitney exact two-tailed U test was performed to com-

pare variables in subjects with a hemorrhage area above or below the mean for the whole group. A one-way analysis of variance performed with the Dunnett correction was used to make pairwise comparisons between IAR measurements by using each detection method. The association between variables was assessed by using the linear least-squares regression. In each case, significance was assumed at a P value of less than .05.

Figure 2

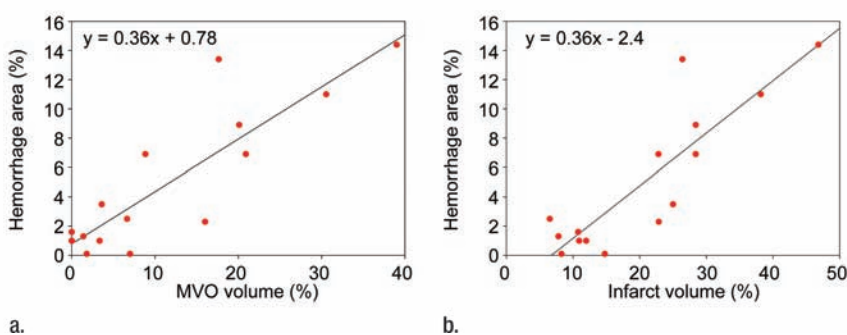


Figure 2: Graphs show correlation between extent of myocardial hemorrhage derived from quantitative $T2^*$ -weighted map and (a) MVO ($r^2 = 0.75$, $P < .01$) and (b) infarct ($r^2 = 0.76$, $P < .01$) volumes (expressed as percentage of total LV volume).

Results

Cardiac MR was performed at a mean of 3.2 days \pm 2.0 (range, 1–7 days) after PPCI, and imaging was well tolerated by all subjects. The coronary vessels that received intervention were the left anterior descending artery ($n = 7$), right coronary artery ($n = 6$), circumflex artery ($n = 1$), and obtuse marginal artery ($n = 1$). Transmural edema was present in all subjects on the $T2$ -weighted short inversion time inversion recovery images and was in the same anatomic region as the late gadolinium enhancement. No patients had late enhancement or edema in more than one area.

Intramyocardial Hemorrhage after PPCI

The mean area of hemorrhage, as indicated by a $T2^*$ measurement of less than 20 msec, was 5.0% \pm 4.9 (range, 0.1%–14.4%) at the level of the infarct. A value of 5% of the hemorrhage area was therefore considered as the cutoff value for subsequent subgroup analysis. In total, six (40%) of 15 of subjects demonstrated 5% or more hemorrhage after reperfusion (Fig 1). There was a close correlation between the extent of hemorrhage and the MVO ($r^2 = 0.75$, $P < .01$) and infarct ($r^2 = 0.76$, $P < .01$) volumes (Fig 2). A summary of the patient information and cardiac MR-derived indexes, given the extent of hemorrhage, is provided in the Table.

IAR and Myocardial Salvage Assessment in Hemorrhagic Myocardial Infarcts

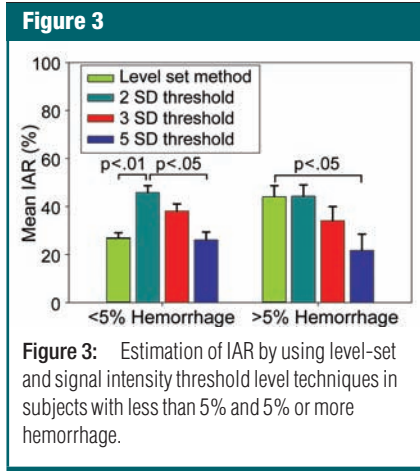
By using the edge detection method, the mean IAR in all subjects was 33.9% \pm 12.0 (range, 20.3%–57.0%). The mean IAR was larger in subjects

Patient Details and Cardiac MR Indexes Grouped by Using Extent of Myocardial Hemorrhage

Characteristic	Hemorrhage <5% ($n = 9$)*	Hemorrhage \geq 5% ($n = 6$)*	P Value
Patient data			
Age (y)	58.1 \pm 10.9	61.2 \pm 6.1	.689
No. of men	7	6	
Time from pain to balloon angioplasty (h)	3.4 \pm 1.7	6.8 \pm 4.7	.181
Time from balloon angioplasty to cardiac MR (d)	3.0 \pm 2.2	3.0 \pm 1.9	.607
Troponin	84 \pm 147	150 \pm 89.5	.026 [†]
Cardiac MR indexes			
LV mass index (g/m ²)	81.3 \pm 15.8	99.2 \pm 18.1	.113
LV end-diastolic volume index (mL/m ²)	72.1 \pm 22.5	81.7 \pm 14.6	.224
LV end-systolic volume index (mL/m ²)	30.3 \pm 11.8	48.7 \pm 15.5	.066
Stroke volume (mL)	81.0 \pm 24.7	61.7 \pm 6.6	.088
Ejection fraction (%)	59.8 \pm 5.4	42.0 \pm 12.0	.018 [†]
MVO (%)	4.5 \pm 5.0	22.8 \pm 10.5	.001 [†]
Infarct (%)	16.7 \pm 5.6	31.8 \pm 8.9	.001 [†]
IAR (level set) (%)	27.0 \pm 6.3	44.1 \pm 11.2	.005 [†]
Myocardial salvage (level set) (%)	40.7 \pm 19.7	14.5 \pm 13.7	.026 [†]

* Data are the mean \pm standard deviation.

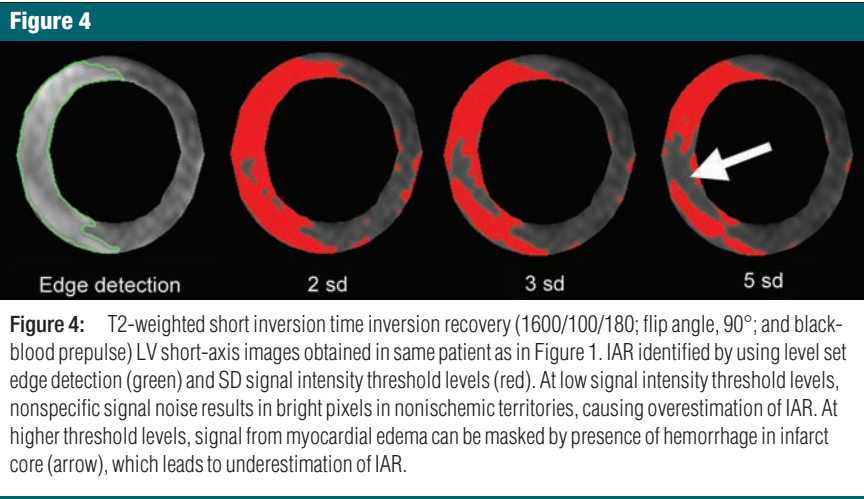
[†] Significant difference by using Mann-Whitney U test.



with 5% or more hemorrhage with a mean size of $44.1\% \pm 11.2$, as compared with $27.0\% \pm 6.3$ in subjects with less than 5% hemorrhage ($P < .01$).

Compared with level-set measurement, a two-SD signal intensity threshold level overestimated the IAR by 69% (45.8% vs 27.0% , $P < .01$) in subjects with less than 5% hemorrhage, while a five-SD threshold level provided the closest agreement (26.1% vs 27.0% , $P = .8$). However, when 5% or more hemorrhage is present, the IAR was underestimated by 50% (21.8% vs 44.0% , $P < .05$) by using the same five-SD threshold level (Fig 3). This underestimation of IAR was a result of diminished T2 signal intensity in the IAR when hemorrhage was present (Fig 4).

Finally, we determined the effect of the level-set and threshold level methods on measurements of myocardial salvage. Owing to the effects of hemorrhage on threshold level–based estimation of IAR, we observed marked variation in the salvage index of patients with hemorrhage across the range of threshold levels as compared with the level-set method (Fig 5). Indeed, estimation of myocardial salvage at three- and five-SD threshold levels becomes unreliable in hemorrhagic infarcts as the apparent IAR becomes smaller than the actual infarct size. It was notable that by using the level-set technique, the mean myocardial salvage index was reduced in subjects with 5% or more hemorrhage with a mean index of $14.5\% \pm 13.7$, as compared with $40.7\% \pm 19.7$ in subjects with less than 5% hemorrhage ($P < .01$).

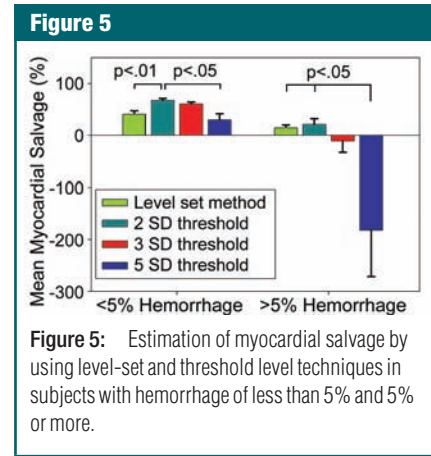


Discussion

Our findings demonstrate the feasibility of using navigator-gated T2*-weighted MR mapping of the heart to quantify the extent of myocardial hemorrhage following infarct reperfusion. Hemorrhage is frequently observed and is associated with large infarcts where MVO is present and is an indicator of poor myocardial salvage. Hemorrhage in the core of the ischemic region causes signal loss on T2-weighted images and boundary detection is required to reliably assess the IAR.

Cardiac MR Imaging of Hemorrhage after Reperfusion

The effects of hemorrhage on T2 relaxation are complex and depend on the form of hemoglobin present (oxyhemoglobin, deoxyhemoglobin, or methemoglobin), the presence of blood degradation products (ferritin and hemosiderin), and the effects of cellular compartmentalization. The patients in this study were imaged 1–7 days after PPCI, when hematoma typically demonstrates marked T2 hypointensity owing to intracellular deoxyhemoglobin and methemoglobin (23). The T2 signal of hemorrhagic myocardial infarction is therefore determined by using the two opposing mechanisms of edema (increased T2 signal) and paramagnetism (decreased T2 signal) (14). The resulting relatively hypointense hemorrhagic core of the infarct seen on T2-weighted images (Fig 5)



shows a close correspondence to the distribution of interstitial hemorrhage on pathologic specimens in humans (11). A more sensitive technique for detecting intramyocardial hemorrhage is to use T2*-weighted gradient-echo sequences, which have an additional dependence on T2' decay owing to magnetic field inhomogeneities (24,25). However, the use of T2*-weighted maps to quantify hemorrhage after PPCI in humans has not been applied, to our knowledge. By using the approach we have developed, it is now possible to compare the extent of hemorrhage with other indexes of ischemia or infarction. Perhaps surprisingly, hemorrhage is common during PPCI and can occur even after short-term coronary occlusion. Antiplatelet drugs and heparin,

which are routinely prescribed periprocedurally, might influence the extent of reperfusion hemorrhage. A study with a larger sample size may also confirm the association between pain-to-balloon angioplasty time and development of hemorrhage.

Hemorrhage after Reperfusion Indicates Diminished Myocardial Salvage

Hemorrhage has been observed in canine models following reperfusion of infarcted myocardium where the extent of hemorrhage is determined by the time delay between coronary artery occlusion and subsequent reperfusion (26). In this model, hemorrhage occurs only in myocardium already markedly compromised at the time of reperfusion, in which tissue necrosis has already developed (12,27) and is not the primary cause of microvascular injury (28). In human studies, qualitative detection of hemorrhage by using cardiac MR following balloon angioplasty for myocardial infarction has been associated with irreversible microvascular damage (24,25). Our data, obtained following PPCI, show that hemorrhage is also an indicator of poor myocardial salvage potential. This reflects the observation that larger infarcts tend to have MVO (29), which predisposes the myocardium to reperfusion hemorrhage.

Effect of Hemorrhage on Estimating the IAR

Accurate measurement of the IAR is required for studies aimed at improving myocardial salvage (30). Cardiac MR techniques for measuring the IAR on T2-weighted images have included manual contouring (29), a half-maximal signal intensity threshold level (8,10), a two-SD signal intensity threshold level with a minimum contiguous area (31), and a three-SD signal intensity threshold level (32). The limitation of using these methods on images with relatively low contrast-to-noise ratio is that noise outside the ischemic territory may be erroneously included in the IAR measurement. Also, our data show that low signal within the infarct core owing to reperfusion hemorrhage may also fall below the signal intensity threshold

level for measurement. A similar issue arises owing to the low signal of MVO demonstrated at late gadolinium enhancement imaging. As there is a contiguous region of myocardial edema following coronary occlusion, it appears appropriate to define the IAR by using a single boundary (13). For our study, we used a level-set image analysis tool that is designed for segmentation of less defined boundaries owing to low contrast or background noise levels (19) and is freely available online (18). A similar segmentation technique has been successfully applied to the higher-contrast images of late gadolinium enhancement to quantify infarct size (33).

Study Limitations

The threshold level for detecting hemorrhage at cardiac MR was not determined on the basis of histologic data, as none of the prospectively recruited patients died. However, there are autopsy case reports demonstrating close histopathologic correlation of the hypointense T2 signal with post-reperfusion hemorrhage in human (11) and animal studies that show that T2 and T2* sequences accurately localize blood products (15,34). Changes in myocardial T2* signal are not specific for hemorrhage. Iron overload shortens T2* signal (20) and the blood oxygen level-dependent effect may also cause subtle changes in T2* signal owing to capillary recruitment in chronically ischemic myocardium (35). None of the subjects in the study were known to have iron overload. Also the blood oxygen level-dependent effect of intracapillary deoxyhemoglobin is likely to be modest in comparison with the paramagnetic effects of macroscopic hemorrhage. Lastly, although nonenhancing myocardium within the infarct is thought to represent MVO (29,36,37), it is possible that the presence of blood products may also contribute to its low signal seen on cardiac MR images (11).

Practical application: Studies performed with cardiac MR to determine the IAR and myocardial salvage should use boundary detection methods for quantification, as arbitrary signal intensity threshold levels are unreliable when hemorrhage is present. Postreperfusion hemorrhage can be assessed

by using T2* mapping and may provide an imaging marker of poor myocardial salvage.

References

1. Bragadeesh T, Jayaweera AR, Pascotto M, et al. Post-ischaemic myocardial dysfunction (stunning) results from myofibrillar oedema. *Heart* 2008;94:166–171.
2. DiBona DR, Powell WJ Jr. Quantitative correlation between cell swelling and necrosis in myocardial ischemia in dogs. *Circ Res* 1980;47:653–665.
3. Jennings RB, Schaper J, Hill ML, Steenbergen C Jr, Reimer KA. Effect of reperfusion late in the phase of reversible ischemic injury: changes in cell volume, electrolytes, metabolites, and ultrastructure. *Circ Res* 1985;56:262–278.
4. Schulz-Menger J, Gross M, Messroghli D, Uhlich F, Dietz R, Friedrich MG. Cardiovascular magnetic resonance of acute myocardial infarction at a very early stage. *J Am Coll Cardiol* 2003;42:513–518.
5. Nilsson JC, Nielsen G, Groenning BA, et al. Sustained postinfarction myocardial oedema in humans visualised by magnetic resonance imaging. *Heart* 2001;85:639–642.
6. Garcia-Dorado D, Oliveras J, Gili J, et al. Analysis of myocardial oedema by magnetic resonance imaging early after coronary artery occlusion with or without reperfusion. *Cardiovasc Res* 1993;27:1462–1469.
7. Boxt LM, Hsu D, Katz J, et al. Estimation of myocardial water content using transverse relaxation time from dual spin-echo magnetic resonance imaging. *Magn Reson Imaging* 1993;11:375–383.
8. Aletras AH, Tilak GS, Natanzon A, et al. Retrospective determination of the area at risk for reperfused acute myocardial infarction with T2-weighted cardiac magnetic resonance imaging: histopathological and displacement encoding with stimulated echoes (DENSE) functional validations. *Circulation* 2006;113:1865–1870.
9. Stork A, Lund GK, Muellerleile K, et al. Characterization of the peri-infarction zone using T2-weighted MRI and delayed-enhancement MRI in patients with acute myocardial infarction. *Eur Radiol* 2006;16:2350–2357.
10. Tilak GS, Hsu LY, Hoyt RF, Arai AE, Aletras AH. In vivo T2-weighted magnetic resonance imaging can accurately determine the ischemic area at risk for 2-day-old nonreperfused myocardial infarction. *Invest Radiol* 2008;43:7–15.
11. Basso C, Corbetti F, Silva C, et al. Morpho-

- logic validation of reperfused hemorrhagic myocardial infarction by cardiovascular magnetic resonance. *Am J Cardiol* 2007;100:1322-1327.
12. Higginson LA, White F, Heggtveit HA, Sanders TM, Bloor CM, Covell JW. Determinants of myocardial hemorrhage after coronary reperfusion in the anesthetized dog. *Circulation* 1982;65:62-69.
 13. Reimer KA, Lowe JE, Rasmussen MM, Jennings RB. The wavefront phenomenon of ischemic cell death. I. Myocardial infarct size vs duration of coronary occlusion in dogs. *Circulation* 1977;56:786-794.
 14. Lotan CS, Miller SK, Cranney GB, Pohost GM, Elgavish GA. The effect of postinfarction intramyocardial hemorrhage on transverse relaxation time. *Magn Reson Med* 1992;23:346-355.
 15. van den Bos EJ, Baks T, Moelker AD, et al. Magnetic resonance imaging of haemorrhage within reperfused myocardial infarcts: possible interference with iron oxide-labelled cell tracking? *Eur Heart J* 2006;27:1620-1626.
 16. Bydder M, Larkman DJ, Hajnal JV. Combination of signals from array coils using image-based estimation of coil sensitivity profiles. *Magn Reson Med* 2002;47:539-548.
 17. Look DC, Locker DR. Time saving in measurement of NMR and EPR relaxation times. *Rev Sci Instrum* 1970;41:250-251.
 18. Cancer for Information Technology. Medical image processing, analysis, and visualization. National Institutes of Health. <http://mipav.nih.gov/>. Accessed April 8, 2008.
 19. Malladi R, Sethian JA. Level set methods for curvature flow, image enhancement, and shape recovery in medical images. In: *Proceedings of Conference on Visualization and Mathematics*. Berlin, Germany: Springer-Verlag, 1995; 329-345.
 20. Anderson LJ, Holden S, Davis B, et al. Cardiovascular T2-star (T2*) magnetic resonance for the early diagnosis of myocardial iron overload. *Eur Heart J* 2001;22:2171-2179.
 21. Reeder SB, Faranesh AZ, Boxerman JL, McVeigh ER. In vivo measurement of T²* and field inhomogeneity maps in the human heart at 1.5 T. *Magn Reson Med* 1998;39:988-998.
 22. Atalay MK, Poncelet BP, Kantor HL, Brady TJ, Weisskoff RM. Cardiac susceptibility artifacts arising from the heart-lung interface. *Magn Reson Med* 2001;45:341-345.
 23. Bradley WG. MR appearance of hemorrhage in the brain. *Radiology* 1993;189:15-26.
 24. Asanuma T, Tanabe K, Ochiai K, et al. Relationship between progressive microvascular damage and intramyocardial hemorrhage in patients with reperfused anterior myocardial infarction: myocardial contrast echocardiographic study. *Circulation* 1997;96:448-453.
 25. Ochiai K, Shimada T, Murakami Y, et al. Hemorrhagic myocardial infarction after coronary reperfusion detected in vivo by magnetic resonance imaging in humans: prevalence and clinical implications. *J Cardiovasc Magn Reson* 1999;1:247-256.
 26. Pislaru SV, Barrios L, Stassen T, Jun L, Pislaru C, Van de Werf F. Infarct size, myocardial hemorrhage, and recovery of function after mechanical versus pharmacological reperfusion: effects of lytic state and occlusion time. *Circulation* 1997;96:659-666.
 27. Kloner RA, Ellis SG, Lange R, Braunwald E. Studies of experimental coronary artery reperfusion: effects on infarct size, myocardial function, biochemistry, ultrastructure and microvascular damage. *Circulation* 1983;68:8-15.
 28. Fishbein MC, Y-Rit J, Lando U, Kanmatsuse K, Mercier JC, Ganz W. The relationship of vascular injury and myocardial hemorrhage to necrosis after reperfusion. *Circulation* 1980;62:1274-1279.
 29. Bogaert J, Kalantzi M, Rademakers FE, Dymarkowski S, Janssens S. Determinants and impact of microvascular obstruction in successfully reperfused ST-segment elevation myocardial infarction: assessment by magnetic resonance imaging. *Eur Radiol* 2007;17:2572-2580.
 30. Janssens S, Dubois C, Bogaert J, et al. Autologous bone marrow-derived stem-cell transfer in patients with ST-segment elevation myocardial infarction: double-blind, randomised controlled trial. *Lancet* 2006;367:113-121.
 31. Friedrich MG, Abdel-Aty H, Taylor A, Schulz-Menger J, Messroghli D, Dietz R. The salvaged area at risk in reperfused acute myocardial infarction as visualized by cardiovascular magnetic resonance. *J Am Coll Cardiol* 2008;51:1581-1587.
 32. Ibanez B, Prat-Gonzalez S, Speidl WS, et al. Early metoprolol administration before coronary reperfusion results in increased myocardial salvage: analysis of ischemic myocardium at risk using cardiac magnetic resonance. *Circulation* 2007;115:2909-2916.
 33. Hsu LY, Ingkanisorn WP, Kellman P, Aletras AH, Arai AE. Quantitative myocardial infarction on delayed enhancement MRI. II. Clinical application of an automated feature analysis and combined thresholding infarct sizing algorithm. *J Magn Reson Imaging* 2006;23:309-314.
 34. Lotan CS, Bouchard A, Cranney GB, Bishop SP, Pohost GM. Assessment of postreperfusion myocardial hemorrhage using proton NMR imaging at 1.5 T. *Circulation* 1992;86:1018-1025.
 35. Wacker CM, Hartlep AW, Pflieger S, Schad LR, Ertl G, Bauer WR. Susceptibility-sensitive magnetic resonance imaging detects human myocardium supplied by a stenotic coronary artery without a contrast agent. *J Am Coll Cardiol* 2003;41:834-840.
 36. Rochitte CE, Lima JA, Bluemke DA, et al. Magnitude and time course of microvascular obstruction and tissue injury after acute myocardial infarction. *Circulation* 1998;98:1006-1014.
 37. Lund GK, Stork A, Saeed M, et al. Acute myocardial infarction: evaluation with first-pass enhancement and delayed enhancement MR imaging compared with 201Tl SPECT imaging. *Radiology* 2004;232:49-57.